Effects of Rosemary Oil (*Rosmarinus Officinalis*) Supplementation on the Fate of the Transplanted Human Olfactory Bulb Neural Stem Cells Against Ibotenic Acid-Induced Neurotoxicity (Alzheimer Model) in Rat

Shaymaa Rezk
Mansoura University Faculty of Veterinary Medicine
Samah Lashen
Mansoura University Faculty of Veterinary Medicine
Mohamed EL-Adl
Mansoura University Faculty of Veterinary Medicine
Gehad E. Elshopakey (gehadelshobaky@yahoo.com)
Mansoura University Faculty of Veterinary Medicine https://orcid.org/0000-0003-2924-9670
Mona M. Elghareeb
Mansoura University Faculty of Veterinary Medicine
Basma M. Hendam
Mansoura University Faculty of Veterinary Medicine
Thomas Caceci
Virginia-Maryland Regional College of Veterinary Medicine
Carlo CenciarelliC
Institute of Translational Pharmacology National Research Council: Istituto di Farmacologia Traslazionale Consiglio Nazionale delle Ricerche
Hany E. Marei
Mansoura University Faculty of Veterinary Medicine

Research Article

Keywords: Alzheimer's disease, Rosemary Oil, Olfactory bulb neural stem cells, Gene expression, Immunocytochemistry

Posted Date: September 17th, 2021

DOI: https://doi.org/10.21203/rs.3.rs-875831/v1

Version of Record: A version of this preprint was published at Metabolic Brain Disease on January 25th, 2022. See the published version at https://doi.org/10.1007/s11011-021-00890-6.

Abstract

Rosemary oil (ROO) is known to have multiple pharmacological effects: it is an antioxidant, an anti-inflammatory, and cytoprotective. In the present study, we examined the effects of ROO on Human olfactory bulb neuronal stem cells (hOBNSCs) after their transplantation into rats, with the ibotenic (IBO) acid-induced cognitive deficit model. After 7 weeks, cognitive functions were assessed using the Morris water maze (MWM). After two months blood and the hippocampus were collected for biochemical, gene expression, and histomorphometric analyses. Learning ability and memory function were significantly enhanced after hOBNSCs transplantation and were nearly returned to normal in the treated group. The IBO acid injection was associated with a significant decline of total leukocyte count (TLC) and a significant increase in total and toxic neutrophils. As well, the level of IL-1β, TNF-α CRP in serum and levels of MDA and NO in hippocampus tissue were significantly elevated, while antioxidant markers (CAT, GSH, and SOD) were reduced in treated tissue compared to controls. The administration of ROO before or with cell transplantation attenuated all these parameters. In particular, the level of NO nearly returned to normal when rosemary was administrated before cell transplantation. Gene expression analysis revealed the potential protective effect of ROO and hOBNSCs via down-expression of R-βAmyl and R- CAS 3 and R-GFAP genes.

Introduction

Alzheimer's disease (AD) is one of the major public health concerns associated with a progressive and irreversible cognitive deficit and memory loss in aged people (Gjoneska et al. 2015). Currently, the European Prevention of Alzheimer's Dementia (EPAD) committee has classified AD as the most widespread neurodegenerative disease, and its prevalence is expected to double over the next 20 years (Ritchie et al. 2016).

The extracellular aggregation of an amyloid-β peptide (Aβ) as senile plaque and the intraneuronal deposition of neurofibrillary tangles owing to abnormal hyperphosphorylation of tau protein, massive cholinergic neuronal death, an inflammatory cascade, and oxidative stress all represent specific neuropathological features of AD (Alipour et al. 2019). The hippocampus is most vulnerable to these pathological alterations and affected than other areas of the brain (Giraldo et al. 2014). Until now, all the drugs available for AD only relieve clinical symptoms but are unable to prevent progression or to replace the degenerated neurons (Cummings et al. 2014). Consequently, the development of novel therapies to alleviate AD pathologies, inhibit neuronal death, replace dead neurons, eliminate toxic deposits, and provides a better niche for remaining cells are very necessary.

Traditional medicine has become more highly regarded in the past few last decades. Several plant materials are rich in natural antioxidants (Abu-Al-Basal 2010). Rosemary (*Rosmarinus officinalis*) is one of the plants that are widely used around the world as a potent source of natural antioxidants. The efficacy of rosemary as a natural antioxidant is principally attributed to its chemical constituents, including carnosic acid, carnosol, 1,8-cineole, α-pinene, β-pinene, diterpenes, and myrcene-rich essential

oils (NGO et al. 2011). Several studies have demonstrated the therapeutic and pharmacological effects of rosemary essential oil, as anti-nociceptive, anti-inflammatory agent, and cognition-enhancing (Rasoolijazi et al. 2015).

Over the past few years, stem cell-based therapy has been tested in both animal models and clinical trials and has become a potential novel approach for several human diseases, such as autoimmune diseases, and neurodegenerative diseases (Ge et al. 2018).

In AD, several reports have shown improvement in cognitive and memory performances in rats with an AD model after their transplantation with stem cells (McGinley et al. 2018). Among various stem cells, the human adult olfactory bulb neural stem cell (hOBNSCs) provides a potential source for autologous stem cells, while avoiding the ethical issues involved in the use of human embryos (Casalbore et al. 2009).

The therapeutic potential of the hOBNSCs for treating many neurodegenerative diseases such as AD (Marei et al. 2015a), Parkinson (Marei et al. 2015b), and spinal cord injury (Marei et al. 2016), as well as their ability to survive and differentiate into neuronal cell types after transplantation has been established in many of our previous studies (Marei et al. 2015a) (Marei et al. 2015b) (Marei et al. 2016).

The ibotenic acid (IBO) induced AD model has been chosen for this study as intrahippocampal injection of IBO in rats produces nearly the same symptoms and pathological changes that are seen in humans with AD (Karthick et al. 2016a). The present study was thus performed to determine whether rosemary oil (ROO) can alleviate effects on the hippocampus and enhance the differentiation of hOBNSCs into different neuronal linages that might replace damaged neurons resulting from the IBO injection, and to determine the best time for administration of ROO (before hOBNSCs transplantation or concurrently with it).

Materials And Methods

Preparation of oil extract

Rosemary (R. officinalis L.) essential oil used in this work was kindly extracted by the Department of Botany, Faculty of Science, Mansoura University (Mansoura, Egypt). The oil extraction was performed using hydrodistillation process following the described protocol by Tigrine-et al,(Tigrine-Kordjani et al. 2012) and the oil was kept at room temperature till be used. As described by manufacturer, the rosemary oil contained about 32.5% 1,8-cineole, 13.7% α-pinene, 11.3% β-pinene 15.2% p-cymene, 12.2% camphene, 8.6% camphor and 6% of other unidentified compounds.

Animals

Fifty adult male rats (Sprague Dawley strain, 3 months old and 200–250g weight) were used in this study. They were housed in suitable cages (5 rats/cage) under standard hygienic environmental conditions (12h light/12h dark cycle, 25±5^{O}C, and 65% humidity) and freely supplied with a balanced diet

and clean water. The protocol of this experiment was performed according to the ethical committee Guidelines of Faculty of Veterinary Medicine, Mansoura University (Approval number; R/4/307/2019).

Study design

The rats were randomly divided into five groups (10 rats /group) as follows: Group I: control group; no manipulation was received. Group II: IBO–model group; bilaterally intra-hippocampus injected with IBO acid (4 µL). Group III: cell-only group; bilaterally intra-hippocampus injected with IBO acid (4 µL) followed by bilateral intra-hippocampus transplantation of hOBNSCs (4 µL) 22days after IBO acid injection. Group IV: cell + rosemary oil (ROO) before transplantation; injected of IBO acid as in the 2nd group, followed by rosemary oil administration (30mg/kg) by stomach tube at on the 7th day and once a day thereafter for 2; this was then followed with hOBNSCs transplantation on the 22nd day as in the third group. Group V: cells with rosemary oil (ROO) concurrently at transplantation; injected the IBO as in the 2nd group 22 days after hOBNSCs transplantation as in group III and rosemary oil administration (30mg/kg) once a day for 2 weeks

Human olfactory bulb neural stem cells (hOBNSCs) isolation and culture

The hOBNSC were isolated and cultured according to the methods described by Casalbore et al(Casalbore et al. 2009).This step was explained in detail in our previous studies (Marei et al. 2015a) (Marei et al. 2015b) (Marei et al. 2016). The olfactory bulbs were collected from six adult patients (39-45 years) undergoing craniotomy at the Institute of Neurosurgery, Catholic University, Rome, Italy. Informed consent was received according to the Ethical Committee protocols of the Catholic University.

Immunocytochemical assessment

Immunostaining of the cells' composition was performed with appropriate specific antibodies to evaluate the cells' multipotentiality, using the method published by Pagano et al., (Pagano et al. 2000). The primary antibodies used (all from Sigma-Aldrich) were anti-Nestin (1:200, rabbit, for undifferentiated neural stem cells), anti-beta tubulin III (1:100, rabbit, for immature neurons), anti-MAP2 (1:200, rabbit, for mature neurons), anti-GFAP (1:400, mouse, for astrocytes) and anti NG2 (1:100, rabbit, for oligodendrocyte progenitors). The secondary antibodies (also from Sigma-Aldrich) were tetramethylrhodamine isothiocyanate [(TRITC), 1:200, anti-rabbit, anti-mouse, and Fluorescein iso-thiocyanate (FITIC), 1:200, anti-rabbit, anti-mouse. After that, the culture was washed and incubated for 15 min with 4, 6-diamidino2 phenyl indole dihydrochloride [(DAPI), nuclear stain, 1mg/ml, and then examined with FluorsaveTM [Calbiochem; La Jolla, CA, USA].

Morris water maze test (MWMt)

After acclimatization to the environment for one week, the rats were subjected to the Morris water maze to assess spatial memory and learning. The methodology of this test was completely

explained by (Vorhees and Williams 2006). The animal's behavior, the escape latency time (time needed to reach to platform), and time in the target quadrant (quadrant time) were tracked and measured with a digital camera. The scores were recorded on the 6^{th} day after training (before IBO injection) and at the end of the study (before sample collecting with one week).

IBO acid-induced memory deficient rat model

Memory deficient model was performed by bilateral IBO acid (Sigma, St. Louis, MO) injection into the rat's hippocampus. IBO acid was dissolved in 10mM artificial cerebrospinal fluid (CSF) at a concentration of 8 mg/ml (Karthick et al. 2016b). The surgery protocol was the same as that explained in our previous study (Marei et al. 2015a). To anesthetize the rats, a mixture of ketamine (80mg/kg body weight) and Xylazine (10mg/kg body weight) was intraperitoneally administered. Each rat was carefully placed in a stereotactic frame under complete aseptic conditions. Intra-hippocampus injection of 4 µL of IBO acid solution was made slowly over 5 minutes using a 10 µL Hamilton syringe (coordinate, ML: 2.5 mm, AP: 3.5 mm, and VD: 2.7 mm relative to the bregma) according to the brain atlas of Paxinos and Watson (Paxinos and Franklin 2001). Following the injection, the skin was sutured, and the rats were returned to their cages when fully recovered from anesthesia.

hOBNSCs transplantation

Animals in groups III, IV, and V were subjected to hOBNSCs transplantation surgery on the 22nd day after IBO injection. A Trypan blue exclusion test was used immediately before cell transplantation to detect cell viability (not less than 95 % viability) under a phase-contrast microscope(Glass et al. 2012). The total cell number was calculated with a hemocytometer then the cells were suspended in artificial CSF (60,000 cells/µL). Animals were re-anesthetized and 4 µL of cell suspension was transplanted (2 µL for each side) into each rat using a 10 µL Hamilton syringe at the same coordinates mentioned above. The immune suppressor cyclosporine (Sandimmune®) was injected daily (10 mg/kg/S.C.) one day before cell grafting and throughout the experiment's course.

Sample collection

Samples were concurrently collected from each group 11 weeks after IBO acid injection (8 weeks after cell transplantation). Blood samples were collected through cardiac puncture and divided into 2 parts. The first part was collected into EDTA tubes for total leukocyte count (TLC) and differential leukocyte count (DLC). The second part was collected into plain clean centrifuge tubes and allowed to clot at room temperature for 30 min. The serum was separated by centrifugation at 3500 r. p.m. for 10 min then aspirated by automatic pipette and kept frozen at −80 °C for further estimation of cytokine levels. After that, rats were euthanized, and their brains were dissected. The hippocampus was collected from each rat. Tissue samples were divided into three groups. The 1st group was fixed in neutral formalin 10% (48hrs) for histological examination and morphometric analyses; the 2nd group was preserved in Trizol Reagent (Invitrogen, UK) for gene expression analyses and the 3rd group was homogenized and cold

centrifuged; the supernatants were separated and carefully collected into clean sterile tubes to be used in the evaluation of antioxidants and oxidative stress parameters.

Total leukocyte and differential leukocyte count

Blood samples were diluted with Turks' solution (1:20) for manual calculation of TLC under a light microscope (10x lens) using a hemocytometer according to the method of Wintrobe, 1993 As well, a thin blood film was spread on a glass slide, air-dried and fixed in absolute methanol (100%). The dried slides were stained with Giemsa stain. Later, 200 leukocytes cell on each slide were examined under an oil immersion lens (100 x) and used to determine the absolute count of normal neutrophils, toxic neutrophils, total neutrophils, lymphocytes, and monocytes. Neutrophil lymphocyte ratio (NLR) and lymphocyte monocyte ratio (LMR) were calculated according to ([CSL STYLE ERROR: reference with no printed form.]).

Serum cytokines and C-reactive proteins (CRP)

Serum tumor necrosis factor-alpha (TNF-α) and IL-1β concentrations were measured in serum using ELISA, with ready-made commercial kits purchased from Quantikine Co. (USA). CRP was estimated according to the standard protocol of ELISA ready-made kits obtained from Cobas Co. (USA).

Antioxidants and Oxidative stress parameters

Catalase (CAT) activity was assessed in hippocampus tissues according to the method of Claiborne (Greenwald 1985), while glutathione (GSH) level was determined according to the method of (Jollow et al. 1974) and superoxide dismutase activity (SOD) was measured according to (MARKLUND and MARKLUND 1974).Furthermore, Malondialdehyde (MDA) level was determined according to the technique of (Todorova et al. 2005).Total Nitric oxide (NO) levels were converted to stable nitrite/nitrate and determined using Greiss' reagent according to the method of (Miranda et al. 2001) with the modification of using zinc sulfate for protein precipitation.All other parameters were determined in hippocampus tissue homogenates using a spectrophotometer (Lambda EZ201; Perkin Elmer).

Total RNA extraction and gene expression analysis

RNA was totally extracted from the hippocampus specimens with the use of Trizol Reagent (Invitrogen, UK) following the procedures of the manufacturer. The concentration of RNA and purity were checked with a "Q5000" Quawell nanodrop spectrophotometer (USA). The integrity of RNA was also assessed by gel electrophoresis. An equivalent of 2mg of RNA was transferred to cDNA with a kit supplied from Intronbio, South Korea (Hisenscript^{TM} cDNA synthesis kit) according to the instructional manual.

Quantitative real-time PCR (qRT-PCR) was performed on a Rotor-Gene Q cycler (Qiagen, Heidelberg, Germany), using QuantiTect SYBR Green PCR kits (Qiagen, Heidelberg, Germany). The sequences of the

primers used in this study are shown in Table 1. The ß-actin gene acted as an internal control for normalizing expression levels of the target genes(Livak and Schmittgen 2001). The total volume of the reaction is 20 µL, which contained 10 µL 2x SensiFast SYBR, 3 µL cDNA, 5.4 µl for H2) (distilled water), and finally 0.8 µl of each gene-specific primer. The amplification cycling conditions were: 95 ^{o}C for 10 min then 40 cycles of 94 ^{o}C for 40 sec; 55 ^{o}C for 30 sec is the optimum temperature for annealing of the chosen primers; then elongation for 30 sec at a temperature of 72 ^{o}C and again at 72 ^{o}C for final elongation over 10 min. At the end of the amplification cycle, a melting curve was created after completion of the amplification phase; the relative expression analysis of target genes was complete using the $2^{-\Delta\Delta Ct}$ procedures (Pfaffl 2001).

Histomorphometric analyses

Formalin-fixed hippocampus samples were processed for paraffin wax embedding by dehydration in ascending grades of ethanol (50, 70, 80.95, 100,100/1hr for each), then cleared in two changes of xylene (1hr/each); they were paraffin wax impregnated and embedded, sectioned (5 µm) with a rotatory microtome and mounted on coated glass slides. The mounted sections were stained with Hematoxylin & Eosin (H&E) stain or cresyl violet stain and examined under a light microscope. For morphometric analysis, morphometric measures were obtained from all groups. Five different samples from five different rats were taken. Three H&E-stained sections from each sample were examined under higher magnification (x400)(Gao et al. 2006). The mean thickness of the pyramidal layer at CA1 and CA3 and the granular layer of the dentate gyrus was measured with an image analyzer. At the same time, the mean number of their viable neurons was also counted.

Statistical analysis

Statistical analysis of the results was performed using SPSS PC (version 19, IBM Analytics, New York, New York, USA). All values were expressed as mean ± SE. The data were analyzed using a one-way analysis of variance (ANOVA) test followed by Tukey's post hoc test for multiple comparisons. Differences were considered statistically significant at $p < 0.05$.

Results

hOBNSCs immune cytochemical assessment

The hOBNSCs remained in an undifferentiated state when cultured in serum-free proliferation media. The cells only proliferated in clusters or aggregated cells known as neurospheres. These neurospheres were separated into single cells using enzymatic digestion accurate. More than 90% of the cells possessed intact cell membranes that excluded trypan blue dye, confirming cell viability for transplantation (Fig.1 a, b). During the growth phase, more than 90% of the cells remained undifferentiated as they give only positive immune staining of nestin (Fig.1c). After one week of differentiation, most of the cells gave

positive immune reactivity for GFAP and MAP2 (Fig.1d, e) and a small number gave positive immune reactivity for NG2 and (Fig.1f) b-Tubulin III (Fig.1g) confirming the multipotency of the cells.

Water maze test

The mean time of latency to the platform was significantly increased in the IBO acid lesioned group (group II) compared to the control group (group I). The latency time was significantly decreased after the transplantation of hOBNSCs compared to group II especially in group IV which nearly reached that of the control one (Table 2).

The mean time that rats spent in the goal quarter (quadrant time) was significantly decreased in the IBO acid lesioned group compared to the control group. The transplantation of hOBNSCs significantly increased the quadrant time compared to the IBO acid lesioned group especially in group IV as it nearly returned to normal with no significant differences between it and the control (Table 2).

Total leukocyte count and differential leukocyte count

Results of Total leukocyte count (TLC) anddifferential leukocyte count (DLC) are depicted in Table 3. TLC showed a significant decline in the IBO-group (group II) when compared to other groups ($P < 0.05$). Whereas rats that received ROO before stem cell transplantation (group IV) exhibited a significant elevation in TLC, followed by the group receiving stem cells only; and those treated with ROO plus cell transplantation ($P < 0.05$) (group III, V). There was no difference in normal neutrophil value among the experimental groups, but IBO-acid induced a significant elevation of Wintrobe, 1993 when compared to controls ($P < 0.05$). Rats that received ROO before or after cell transplantation had significantly reduced levels of these cells, especially, group IV ($P < 0.05$).

The total neutrophil level was significantly higher in the IBO-group and the stem cell group than in controls ($P < 0.05$), but no significant difference was detected when compared to groups IV and V. Moreover, lymphocyte count was significantly lower in the IBO-group (group II) than in controls ($P < 0.05$); but transplantation of stem cells and ROO administration before or after cell transplantation (group III, IV, and V) significantly increased lymphocyte counts compared to IBO-group ($P < 0.05$) (group II). Besides, IBO induced significant a reduction in monocytes in group II and significant elevations in NLR when compared to controls ($P < 0.05$). As well, stem cell transplantation and ROO administration in groups III, IV, and V had lower NLR when compared to the IBO group ($P < 0.05$). However, LMR didn't show any significant difference among the experimental groups.

Serum cytokines and CRP

Results of serum cytokines and CRP measures are depicted in Figure 2. The levels of pro-inflammatory cytokine IL-1β, TNF-α and CRP in the IBO-group (group II) were significantly higher when compared to controls (group I) ($P < 0.05$). However, administration of ROO before or with transplantation of stem cells (group IV and V) significantly reduces these levels in serum when compared to the IBO group ($P < 0.05$). Only the rats injected with stem cells (group III) showed significant decline in TNF-α levels ($P< 0.05$).

Antioxidants and oxidative stress markers

Results of antioxidant and oxidative stress markers in hippocampus tissues are depicted in Table 4. The activity of anti-oxidative markers (CAT, GSH, and SOD) in hippocampus tissues exhibited a significant decrease in the IBO group as well as stem cell groups when compared to controls ($P < 0.05$). The administration of ROO before or with transplantation of stem cells (group IV and V) caused a significant elevation in those markers in comparison with the IBO group ($P < 0.05$) specifically CAT levels. Moreover, MDA, lipid peroxidation marker, and NO levels in the hippocampus showed a significant increase in the IBO group compared to controls ($P < 0.05$). Injection of stem cells alone or with ROO induced a significant decline when compared to controls ($P < 0.05$) and the lowest level was mainly detected in group IV.

Gene expression with real-time PCR

As shown in figure 3, a forty-seven-fold increase in the expression of R-βAmyl was observed in group II in comparison with group I ($P < 0.05$). This was significantly decreased in all studied groups that received stem cells (group III) alone or in combination with rosemary (groups IV, V), reaching the level of group I.

On the other hand, the apoptotic marker, R-caspase-3, showed an eleven-fold increase of expression in group II when compared with the control group which was the highest group ($P < 0.05$). Meanwhile, expression of cas3 was significantly decreased in groups III and V when compared with the control group ($P < 0.05$), followed by group IV which was similar in expression to the group I with non-significant differences between both groups ($P < 0.05$).

Similarly, the expression of RGFAP showed a significant increase in expression by twenty-two-fold in group II compared to group I ($P < 0.05$). Conversely, the expression of RGFAP was significantly decreased in groups III, IV, V like the group I.

Furthermore, the mean mRNA expression of the HGFAP was increased in group III by 5-fold compared with group I ($p<0.05$), while group IV showed a significant increase in expression of the HGFAP gene by almost 2.5-fold compared with group I ($P < 0.05$). Meanwhile, group II showed the least expression of HGFAP compared with other groups ($P < 0.05$). The expression of HGAP in both groups IV and V showed a non-significant difference between both groups ($P < 0.05$).

Besides, the expression of HMAP2 showed the highest expression in group IV with a thirteen-fold increase in expression when compared with group I ($P < 0.05$). Both groups III and V showed similar expression of HMAP2 ($P < 0.05$), which was still a significant increase in comparison with both groups I and II ($P < 0.05$). Both groups III and V showed a nearly 15-fold expression of HCNP-1 in comparison with group I ($P < 0.05$), while groups IV and II showed nearly the same level of expression as the group I ($P < 0.05$).

Histomorphometric results

The light microscopic examination of the H&E-stained section of the control group (I) exhibited the normal histoarchitecture of the hippocampus. It comprised two major interlocking c-shaped parts, which are the hippocampus proper (CA1, CA2, and CA3) and the dentate gyrus (DG) (Fig.4-a). In the current study only CA1 (Fig.4), CA3 (Fig.5), and the dentate gyrus3 (Fig.6) were subjected to examination as CA2 is poorly defined and small. Both CA1 and CA3 were arranged in three layers; polymorphic, pyramidal, and molecular. The pyramidal layer of CA1 (Fig.4-(1a, 1b)) and CA3 (Fig.5-(1a, 1b)) was the principal layer that contained pyramidal neurons with light vesicular nuclei, scattered astrocytes, and scattered oligodendrocytes. Cresyl violet stained sections through these pyramidal neurons revealed a rim of violet staining Nissl granules forming cap on neurons.

H&E-stained sections from the ibotenic acid-lesioned group (II) revealed that the pyramidal layer appeared loose with a significant decrease in thickness (Fig.4, 5- (6)) and numbers (Fig.4, 5-(7)) of their viable neurons compared to the control group (I); nearly all the pyramidal neurons in CA1 (Fig.4-(2a, 2b)) and CA3 (Fig.5-(2a, 2b)) appeared shrunken and deeply eosinophilic with pyknotic or completely lost nuclei. The density of the Nissl granules was markedly decreased or completely depleted in the pyramidal neurons using cresyl violet stain. Massive gliosis and widely spread congested blood capillaries were detected in the molecular and polymorphic layers.

The pyramidal layer at CAI retained some of its normal histology in a group (III) (Fig.4-(3a, 3b)) and returned to normal when the rosemary oil was given before (group IV) (Fig.5-(4a, 4b)) or with the cell transplantation (group IV) (Fig.4-(5a, 5b)). The number of viable pyramidal neurons was significantly increased after hOBNSCs transplantation compared to the ibotonic acid–lesioned group (Fig.4-(7)), especially in groups IV and V as there is no significant difference between them and the control group.

The histoarchitecture restoration in CA3 was more readily detected in a group (IV) (Fig.5-(4a, 4b)) as the thickness (Fig.5-(6)) and the number (Fig.5-(7)) of intact pyramidal neurons nearly returned to the normal. On other hand, some of the dark shrunken neurons were still detected in a group (III) (Fig.5-(3a, 3b)) and group (V) (Fig.5-(5a, 5b)) and the total number of their viable neurons (Fig.4-(7)) was still significantly decreased compared to the control one (group. I); however, it was significantly increased compared to group (II). The dentate gyrus was formed of three layers; the molecular, granular, and polymorphic layers (Fig.4-(1)).

The granular layer is considered the principal layer of the dentate gyrus and is formed of densely packed granular cells. The superficial part of this layer included mature small rounded granular cells with light vesicular nuclei, while the subgranular zone contained immature neurons with oval dark nuclei (Fig.6-(1a, 1b)). The Cresyl violet stain of the granular layer appeared as blue cells with light vesicular nuclei surrounded by violet Nissl granules. The granular layer in the IBO acid lesioned group appeared disorganized and with significant decreases in thickness and numbers of mature granular cells compared to the control group (Fig.6-(2a, 2b)). Massive gliosis and widely spread congested blood capillaries were detected in the molecular and polymorphic layers. The number of mature granular cells was nearly returned to the numbers of the normal group only in the group (IV) (Fig.6-(4a, 4b)), since in group (III)

(Fig.6-(3a, 3b)) and group (V) (Fig.6-(5a, 5b)) the number of the mature granular cells still significantly decreased compared to group (I); however, they were significantly increased compared to group (II) (Fig.6-(7)).

Discussion

The injection of IBO in the hippocampus was associated with up-regulation in the activity of caspase-3 resulting in oxidative stress, astrocytosis, and amyloid-beta accumulation (Vargas et al. 2010). The histological alteration following IBO administration is similar to the histopathological events seen in the brain of patients with AD (Marei et al. 2015a). We used hOBNSCs that have been reported in many previous studies for their ability to differentiate into different neuronal and glial elements *in vitro* (Marei et al. 2015a)(Marei et al. 2015b)(Marei et al. 2016). Thus combining complementary strategies might be required to enhance the proliferation and differentiation of hOBNSCs in this hostile environment. Based on these findings, our study was designed to investigate whether hOBNSCs alone have the ability to survive, differentiate and replace all damaged neurons or need further assistance by adding ROO as an anti-inflammatory and antioxidant substance (Rašković et al. 2014).

Routine peripheral blood parameters could be new inflammatory markers associated with the inception and prognosis of CNS diseases (Pikija et al. 2018). Our results showed that TLC, lymphocytes, and monocytes significantly declined while NLR, total and toxic neutrophils were significantly elevated in IBO-group. These findings agreed with those of (Dong et al. 2019) who speculated that a higher neutrophil count and NLR could be a favorable conducive diagnostic biomarker for AD.

Additionally, IL-1β and TNF-α are the pro-inflammatory cytokines, generated from microglia and astrocytes (Zuliani et al. 2007) and are involved in the phosphorylation process, the key pathogenic event of AD, as it can cross the blood-brain barrier causing neurodegenerative changes (Li et al. 2003). On the same line of our results (Swardfager et al. 2010) a significantly higher concentration of IL-6, TNF-α, IL-1 β, TGF- β, IL-12, and IL-18 was observed in peripheral blood of AD subjects. The elevation of inflammatory mediators and CRP in the current study may be correlated to activation of astrocyte and microglia by potential damage in hippocampus tissue (amyloid plaques and neurofibrillary tangles) (Venegas and Heneka 2017). After activation, astrocytes enhance the production of ROS and NO, release of TNF-α, IL-1 β, and IL-6, and increase GFAP expression (Palpagama et al. 2019). Actually, the up-regulation of GFAP expression is commonly considered as a distinctive feature of neuroinflammation in many neurodegenerative conditions, including AD(Millington et al. 2014). Similar to our findings, Stoltenberg-Didinger et al. (Stoltenburg-Didinger et al. 1996) investigated that the expression of R-GFAP was increased after the exposure to IBO, a potent neurotoxic substance, which also accompanied an increase in the number of glial cells which express these signals. The histological image of the hippocampus of group II in the current study also exhibited massive gliosis which was detected in the molecular and polymorphic layers of the hippocampus.

Rosmarinic acid from *R. officinalis* is recognized as a tool in the treatment of inflammation and oxidative stress (Rašković et al. 2014) in neurodegenerative diseases. In our study, we investigated the protective effects of ROO on inflammatory responses and oxidative stress in the case of AD. Our results showed that administration of ROO before or after cell transplantation significantly increases lymphocyte count and TLC, while reducing NLR, toxic, and total neutrophil counts. Similar to our findings, neutrophils and monocytes were dramatically decreased; but the levels of lymphocytes and eosinophils were increased in rabbits treated with *R. officinalis* L. extract after prolonged exposure to lead (Mohamed et al. 2016).

Our experiments also demonstrated an anti-inflammatory activity of ROO even when administrated before or with transplantation of stem cells, compared to IBO group. Similarly, cineole administration significantly inhibited cytokine release from blood cells (IL-1β, TNFα, IL-4, IL-5, IL-6, and IL-8) with minor effects on chemotactic cytokines (Juergens et al. 2004).

In the current study, a forty-seven-fold increase in the expression of RAmyl was detected in group II (IBO acid group) in comparison with the control group. As mentioned above, the accumulation of Aβ resulted in activation of astrocytes. The activated astrocytes enhance the production of ROS. Therefore, Aβ is linked with the formation of ROS and induction of oxidative stress that occurs in the case of AD (Tillement et al. 2010).

The significant reduction in antioxidant levels (GSH, SOD, CAT) corroborates the idea that oxidative stress is the early event that has a crucial role in the disease progression (Ansari and Scheff 2010). Similar to our findings, IBO has been reported to exhibit toxicity through the increasing activity of NOS and the production of nitric oxide levels (Karthick et al. 2016c). Additionally, the reduction in GSH, SOD, and CAT levels may be linked to loss of neurons in AD (Bains and Shaw 1997) and increasing the free radical load, which triggers oxidative stress (Bains and Shaw 1997). Moreover, in our study, the hippocampal activities of antioxidant molecules were significantly restored with ROO administration, compared to the IBO or cell treated groups. This was attributed to the active component of rosemary oil (1,8-cineole, α-pinene, and β-pinene and myrcene-rich essential oils) exhibiting greater free radical scavenging activity (NGO et al. 2011).

Furthermore, clinical data demonstrate that a relationship exists between apoptosis, Aβ, and ROS. Aβ could serve as an extracellular signal molecule for caspase-3 activation (Choi et al. 1988), meanwhile, ROS can act as a potent intrinsic stimulus for caspase-3 (Redza-Dutordoir and Averill-Bates 2016). In the current study, the up-regulation of the caspase-3 gene in group II indicated the apoptotic effects of IBO acid on rat's hippocampus tissues. The findings of Kamelia et al(Kamelia et al. 2017) indicated that the accumulation of amyloid-beta exhibited overexpression of caspase-3.

The histological findings and morphometric analysis of the hippocampus confirmed the neurotoxic effects of IBO as the numbers of viable pyramidal neurons at CA1 and CA3 or the number of mature granular cells were significantly decreased compared to the control group. Our results are in harmony with the results of (Karthick et al. 2016c) who reported that a significant histological alteration associated with a significant increase in dead neurons was detected at CA1 and CA3 after IBO induction. The results

published by (Rodríguez et al. 2008)also exhibited that the dentate gyrus of the hippocampus in AD was disorganized and the numbers of mature granular cells was significantly decreased as the newly generated neurons don't become mature in AD. Our antioxidant and gene expression data indicate that the administration of ROO especially before cell transplantation quickly ameliorate the neurotoxicity of IBO injection with hOBNSCs alone or when given concurrently with the cells.

The expression of neuron markers as MAP2 can be used for neural verification and played a role in the stability of axons and neuronal cell bodies through the differentiation process (Kermani et al. 2008). In the hippocampus, the expression of MAP2 was mainly detected in the dendrites of pyramidal neurons and dendrites of granular cells in the dentate gyrus (Kermani et al. 2008). In the current study, the highest expression of hMAP2 was detected in group IV (administrated ROO before cell transplantations). At the same time, the histomorphometric analyses are in harmony with the expression of hMAP2 as the mean number of viable pyramidal neurons at CAI and CA3 or the mean number of mature granular cells was the highest in group IV. The neuroprotective effect of ROO is likely similar to the effect of nerve growth factor (NGF) and it can be hypothesized that the mechanism of the effect of ROO on hOBNSCs might be attributed to NGF-mediated signaling pathways like PI3K/AKT, protein kinase C (PKC) and ERK1/2, which activity is associated with the survival of existing cells and neuronal differentiation (Vaudry et al. 2002). Besides that, the administration of ROO before cell transplantation was associated with a high elevation of antioxidant levels that provide a suitable environment for the hOBNCs to differentiate towards mature neurons. Our results are run parallel with the results of (Villareal et al. 2017) who showed that the expression of Gap 43 protein (a marker of neuronal outgrowth elongation) was up-regulated when PC12 cells were treated with *Rosmarinus officinalis* essential oils, with significant increase in the acetylcholine enzyme activity. Also, MDA and NO levels, and caspase-3 expression were still elevated after hOBNSCs transplantation without ROO compared to the control group resulting in the highest expression of hGFAP was detected in group III.

The amelioration of astrocytosis, beta-amyloid accumulation, and TNF elevation in group III (transplanted with cell only) are not fully understood but may be attributed to the release of some diffusible bioactive trophic factors from the hOBNSCs itself that may decrease many of these neurotoxic substances and so enhance survival and differentiation; or it may be attributed to the increase in the expression of h GFAP in this group, as normal astrocytes have a higher capacity for the production and storage of GSH compared to neurons. Subsequently, they can protect the newly formed neurons from oxidative stress by releasing GSH into the surrounding environment(Baxter and Hardingham 2016). Furthermore, astrocytes also play a role in the degradation and clearance of Aβ through the expression of different types of proteases that are involved in the cleaving of Aβ (Redza-Dutordoir and Averill-Bates 2016).

Loss of neurons at CA1, CA3, and dentate gyrus after intra hippocampus injection with IBO was associated with a progressive decline of cognitive function (Terry and Davies 1980). The behavioral deficit aspect of this model was our main interest. In the current study, the main latency time and quadrant time in the IBO group were significantly increased and decreased respectively compared to the control group; that confirmed that IBO administration is associated with impairment of spatial memory

and cognitive functions. The enhancement in these times was detected after cell transplantation but nearly reached normal when ROO was given before cell transplantation. These results confirm the definitive objective of hOBNSCs transplantation, which is the achievement of cognitive functional recovery. The improvement in the learning and memory function in the current experiment was mostly detected in group IV as this group possesses the highest antioxidant capacity, the lowest inflammatory cytokines, and the lowest expression of caspase and amyloid-beta aggregation.

Conclusion

Taken together the histological, biochemical and gene expression and behavioral findings are strongly suggestive of the administration of ROO before cell transplantation enhances these cells to fast differentiation and integration with the neighboring cells than when given concurrently with the cells and further that administration of ROO before cell transplantation is a promising candidate for cell-based therapy for AD.

Abbreviations

AD, Alzheimer's disease; ROO, rosemary oil; IBO, ibotenic acid; hOBNSCs, Human olfactory bulb neural stem cells; TLC, total leukocyte count; TNF-α, tumor necrosis factor alpha; IL-1β, Interleukin-1β; MDA, Malondialdehyde; NO, Nitric oxide; GSH, Reduced glutathione; SOD, Superoxide dismutase; CAT, Catalase.

Declarations

Acknowledgments: We acknowledge the provision of the human olfactory bulb neural stem cells from Dr. Carlo Cenciarelli, Dept. of Biomedical Sciences, Institute of Translational Pharmacology-CNR, Rome, Italy.

Author Contributions: S.R and S.L, Conceptualization & Visualization; **S.R, S.L, M.E, G.E.E, M.M.E and B.M.H,** Validation & Methodology; **S.R, M.E, G.E.E, M.M.E and B.M.H,** Resources, Data curation and analysis & Writing the original draft; **T.C, C.C and H.E.M,** Supervision; **S.R** Writing—editing; **G.E.E,** Review & prepare manuscript for publication. All authors read and approved the final manuscript.

Data Availability Statement: All data are included in the submitted manuscript.

Conflict of Interest: The authors declare no conflict of interest.

Funding: The present work was self-funding study.

The present research does not involve human participants. All animal procedures were conducted according to the ethical committee Guidelines of Faculty of Veterinary Medicine, Mansoura University (Approval number; R/4/307/2019).

Consent to Participate: Not applicable.

Consent for Publication: Not applicable.

References

1. Abu-Al-Basal MA (2010) Healing potential of Rosmarinus officinalis L. on full-thickness excision cutaneous wounds in alloxan-induced-diabetic BALB/c mice. Journal of Ethnopharmacology 131:443–450. https://doi.org/10.1016/j.jep.2010.07.007
2. Alipour M, Nabavi SM, Arab L, et al (2019) Stem cell therapy in Alzheimer's disease: possible benefits and limiting drawbacks. Molecular Biology Reports 46:1425–1446. https://doi.org/10.1007/s11033-018-4499-7
3. Ansari MA, Scheff SW (2010) Oxidative stress in the progression of alzheimer disease in the frontal cortex. Journal of Neuropathology and Experimental Neurology 69:155–167. https://doi.org/10.1097/NEN.0b013e3181cb5af4
4. Bains JS, Shaw CA (1997) Neurodegenerative disorders in humans: The role of glutathione in oxidative stress-mediated neuronal death. Brain Research Reviews 25:335–358
5. Baxter PS, Hardingham GE (2016) Adaptive regulation of the brain's antioxidant defences by neurons and astrocytes. Free Radical Biology and Medicine 100:147–152
6. Casalbore P, Budoni M, Ricci-Vitiani L, et al (2009) Tumorigenic potential of olfactory bulb-derived human adult neural stem cells associates with activation of TERT and NOTCH1. PLoS ONE 4:. https://doi.org/10.1371/journal.pone.0004434
7. Choi DW, Koh -y. J, Peters S (1988) Pharmacology of glutamate neurotoxicity in cortical cell culture: Attenuation by NMDA antagonists. Journal of Neuroscience 8:185–196. https://doi.org/10.1523/jneurosci.08-01-00185.1988
8. Cummings JL, Morstorf T, Zhong K (2014) Cummings, Jeffrey L_Alzheimer's_drug development candidates failures_2014. 1–7
9. Dong X, Nao J, Shi J, Zheng D (2019) Predictive Value of Routine Peripheral Blood Biomarkers in Alzheimer's Disease. Frontiers in Aging Neuroscience 11:332. https://doi.org/10.3389/fnagi.2019.00332
10. Gao Y, Bezchlibnyk YB, Sun X, et al (2006) Effects of restraint stress on the expression of proteins involved in synaptic vesicle exocytosis in the hippocampus. Neuroscience 141:1139–1148. https://doi.org/10.1016/j.neuroscience.2006.04.066
11. Ge M, Zhang Y, Hao Q, et al (2018) Effects of mesenchymal stem cells transplantation on cognitive deficits in animal models of Alzheimer's disease: A systematic review and meta-analysis. Brain and Behavior 8:1–10. https://doi.org/10.1002/brb3.982
12. Giraldo E, Lloret A, Fuchsberger T, Viña J (2014) Aβ and tau toxicities in Alzheimer's are linked via oxidative stress-induced p38 activation: Protective role of vitamin E. Redox Biology 2:873–877. https://doi.org/10.1016/j.redox.2014.03.002

13. Gjoneska E, Pfenning AR, Mathys H, et al (2015) Conserved epigenomic signals in mice and humans reveal immune basis of Alzheimer's disease. Nature 518:365–369. https://doi.org/10.1038/nature14252
14. Glass JD, Boulis NM, Johe K, et al (2012) Lumbar intraspinal injection of neural stem cells in patients with amyotrophic lateral sclerosis: Results of a phase I trial in 12 patients. Stem Cells 30:1144–1151. https://doi.org/10.1002/stem.1079
15. Greenwald R (1985) CRC handbook of methods for oxygen radical research. CRC Press, Boca Raton Fla.
16. Jollow DJ, Mitchell JR, Zampaglione N, Gillette JR (1974) Bromobenzene-Induced Liver Necrosis. Protective Role of Glutathione and Evidence for 3,4-Bromobenzene Oxide as the Hepatotoxic Metabolite. Pharmacology 11:151–169. https://doi.org/10.1159/000136485
17. Juergens UR, Engelen T, Racké K, et al (2004) Inhibitory activity of 1,8-cineol (eucalyptol) on cytokine production in cultured human lymphocytes and monocytes. Pulmonary Pharmacology and Therapeutics 17:281–287. https://doi.org/10.1016/j.pupt.2004.06.002
18. Kamelia E, Islam AA, Hatta M, et al (2017) Evaluation of caspase-3 mRNA gene expression activity in amyloid beta-induced Alzheimer's disease rats. Journal of Medical Sciences (Faisalabad) 17:117–125. https://doi.org/10.3923/jms.2017.117.125
19. Karthick C, Periyasamy S, Jayachandran KS, Anusuyadevi M (2016a) Intrahippocampal administration of ibotenic acid induced cholinergic dysfunction via NR2A/NR2B expression: Implications of resveratrol against Alzheimer disease pathophysiology. Frontiers in Molecular Neuroscience 9:1–16. https://doi.org/10.3389/fnmol.2016.00028
20. Karthick C, Periyasamy S, Jayachandran KS, Anusuyadevi M (2016b) Intrahippocampal administration of ibotenic acid induced cholinergic dysfunction via NR2A/NR2B expression: Implications of resveratrol against Alzheimer disease pathophysiology. Frontiers in Molecular Neuroscience 9:1–16. https://doi.org/10.3389/fnmol.2016.00028
21. Karthick C, Periyasamy S, Jayachandran KS, Anusuyadevi M (2016c) Intrahippocampal administration of ibotenic acid induced cholinergic dysfunction via NR2A/NR2B expression: Implications of resveratrol against Alzheimer disease pathophysiology. Frontiers in Molecular Neuroscience 9:1–16. https://doi.org/10.3389/fnmol.2016.00028
22. Kermani S, Karbalaie K, Madani SH, et al (2008) Effect of lead on proliferation and neural differentiation of mouse bone marrow-mesenchymal stem cells. Toxicology in Vitro 22:995–1001. https://doi.org/10.1016/j.tiv.2008.02.009
23. Li Y, Liu L, Barger SW, Griffin WST (2003) Interleukin-1 mediates pathological effects of microglia on tau phosphorylation and on synaptophysin synthesis in cortical neurons through a p38-MAPK pathway. Journal of Neuroscience 23:1605–1611. https://doi.org/10.1523/jneurosci.23-05-01605.2003
24. Livak KJ, Schmittgen TD (2001) Analysis of relative gene expression data using real-time quantitative PCR and the 2-ΔΔCT method. Methods 25:402–408.

https://doi.org/10.1006/meth.2001.1262

25. Marei HE, Althani A, Rezk S, et al (2016) Therapeutic potential of human olfactory bulb neural stem cells for spinal cord injury in rats. Spinal Cord 54:785–797. https://doi.org/10.1038/sc.2016.14
26. Marei HES, Farag A, Althani A, et al (2015a) Human olfactory bulb neural stem cells expressing hNGF restore cognitive deficit in Alzheimer's disease rat model. Journal of Cellular Physiology 230:116–130. https://doi.org/10.1002/jcp.24688
27. Marei HES, Lashen S, Farag A, et al (2015b) Human olfactory bulb neural stem cells mitigate movement disorders in a rat model of Parkinson's disease. Journal of Cellular Physiology 230:1614–1629. https://doi.org/10.1002/jcp.24909
28. MARKLUND S, MARKLUND G (1974) Involvement of the Superoxide Anion Radical in the Autoxidation of Pyrogallol and a Convenient Assay for Superoxide Dismutase. European Journal of Biochemistry 47:469–474. https://doi.org/10.1111/j.1432-1033.1974.tb03714.x
29. McGinley LM, Kashlan ON, Bruno ES, et al (2018) Human neural stem cell transplantation improves cognition in a murine model of Alzheimer's disease. Scientific Reports 8:1–10. https://doi.org/10.1038/s41598-018-33017-6
30. Millington C, Sonego S, Karunaweera N, et al (2014) Chronic neuroinflammation in Alzheimer's disease: New perspectives on animal models and promising candidate drugs. BioMed Research International 2014:. https://doi.org/10.1155/2014/309129
31. Miranda KM, Espey MG, Wink DA (2001) A rapid, simple spectrophotometric method for simultaneous detection of nitrate and nitrite. Nitric Oxide - Biology and Chemistry 5:62–71. https://doi.org/10.1006/niox.2000.0319
32. Mohamed WAM, Abd-Elhakim YM, Farouk SM (2016) Protective effects of ethanolic extract of rosemary against lead-induced hepato-renal damage in rabbits. Experimental and Toxicologic Pathology 68:451–461. https://doi.org/10.1016/j.etp.2016.07.003
33. NGO SNT, Williams DB, Head RJ (2011) Rosemary and cancer prevention: Preclinical perspectives. Critical Reviews in Food Science and Nutrition 51:946–954
34. Pagano SF, Impagnatiello F, Girelli M, et al (2000) Isolation and Characterization of Neural Stem Cells from the Adult Human Olfactory Bulb. Stem Cells 18:295–300. https://doi.org/10.1634/stemcells.18-4-295
35. Palpagama TH, Waldvogel HJ, Faull RLM, Kwakowsky A (2019) The Role of Microglia and Astrocytes in Huntington's Disease. Frontiers in Molecular Neuroscience 12:1–15. https://doi.org/10.3389/fnmol.2019.00258
36. Paxinos G, Franklin KBJ (2001) Paxinos and Franklin's the Mouse Brain in Stereotaxic Coordinates
37. Pfaffl MW (2001) A new mathematical model for relative quantification in real-time RT-PCR. Nucleic Acids Research 29:45e–445. https://doi.org/10.1093/nar/29.9.e45
38. Pikija S, Sztriha LK, Killer-Oberpfalzer M, et al (2018) Neutrophil to lymphocyte ratio predicts intracranial hemorrhage after endovascular thrombectomy in acute ischemic stroke. Journal of Neuroinflammation 15:319. https://doi.org/10.1186/s12974-018-1359-2

39. Rašković A, Milanović I, Pavlović N, et al (2014) Antioxidant activity of rosemary (Rosmarinus officinalis L.) essential oil and its hepatoprotective potential. BMC Complementary and Alternative Medicine 14:225. https://doi.org/10.1186/1472-6882-14-225
40. Rasoolijazi H, Mehdizadeh M, Soleimani M, et al (2015) The effect of rosemary extract on spatial memory, learning and antioxidant enzymes activities in the hippocampus of middle-aged rats. Medical Journal of the Islamic Republic of Iran 29:
41. Redza-Dutordoir M, Averill-Bates DA (2016) Activation of apoptosis signalling pathways by reactive oxygen species. Biochimica et Biophysica Acta (BBA) - Molecular Cell Research 1863:2977–2992. https://doi.org/10.1016/j.bbamcr.2016.09.012
42. Ritchie CW, Molinuevo JL, Truyen L, et al (2016) Development of interventions for the secondary prevention of Alzheimer's dementia: The European Prevention of Alzheimer's Dementia (EPAD) project. The Lancet Psychiatry 3:179–186
43. Rodríguez JJ, Jones VC, Tabuchi M, et al (2008) Impaired adult neurogenesis in the dentate gyrus of a triple transgenic mouse model of Alzheimer's Ddisease. PLoS ONE 3:. https://doi.org/10.1371/journal.pone.0002935
44. Stoltenburg-Didinger G, Pünder I, Peters B, et al (1996) Glial fibrillary acidic protein and RNA expression in adult rat hippocampus following low-level lead exposure during development. Histochemistry and Cell Biology 105:431–442. https://doi.org/10.1007/BF01457656
45. Swardfager W, Lanctt K, Rothenburg L, et al (2010) A meta-analysis of cytokines in Alzheimer's disease. Biological Psychiatry 68:930–941. https://doi.org/10.1016/j.biopsych.2010.06.012
46. Terry RD, Davies P (1980) Dementia of the Alzheimer Type. Annual Review of Neuroscience 3:77–95. https://doi.org/10.1146/annurev.ne.03.030180.000453
47. Tigrine-Kordjani N, Meklati BY, Chemat F, Guezil FZ (2012) Kinetic Investigation of Rosemary Essential Oil by Two Methods: Solvent-Free Microwave Extraction and Hydrodistillation. Food Analytical Methods 5:596–603. https://doi.org/10.1007/s12161-011-9283-4
48. Tillement J-P, Lecanu L, Papadopoulos V (2010) Amyloidosis and Neurodegenerative Diseases: Current Treatments and New Pharmacological Options. Pharmacology 85:1–17. https://doi.org/10.1159/000259044
49. Todorova I, Simeonova G, Kyuchukova D, et al (2005) Reference values of oxidative stress parameters (MDA, SOD, CAT) in dogs and cats. Comparative Clinical Pathology 13:190–194. https://doi.org/10.1007/s00580-005-0547-5
50. Vargas T, Ugalde C, Spuch C, et al (2010) Aβ accumulation in choroid plexus is associated with mitochondrial-induced apoptosis. Neurobiology of Aging 31:1569–1581. https://doi.org/10.1016/j.neurobiolaging.2008.08.017
51. Vaudry D, Stork PJS, Lazarovici P, Eiden LE (2002) Signaling pathways for PC12 cell differentiation: Making the right connections. Science 296:1648–1649
52. Venegas C, Heneka MT (2017) Danger-associated molecular patterns in Alzheimer's disease. Journal of Leukocyte Biology 101:87–98. https://doi.org/10.1189/jlb.3mr0416-204r

53. Villareal MO, Ikeya A, Sasaki K, et al (2017) Anti-stress and neuronal cell differentiation induction effects of Rosmarinus officinalis L. essential oil. BMC Complementary and Alternative Medicine 17:1–10. https://doi.org/10.1186/s12906-017-2060-1
54. Vorhees C V., Williams MT (2006) Morris water maze: Procedures for assessing spatial and related forms of learning and memory. Nature Protocols 1:848–858. https://doi.org/10.1038/nprot.2006.116
55. Zuliani G, Ranzini M, Guerra G, et al (2007) Plasma cytokines profile in older subjects with late onset Alzheimer's disease or vascular dementia. Journal of Psychiatric Research 41:686–693. https://doi.org/10.1016/j.jpsychires.2006.02.008
56. Wintrobe's clinical hematology. (Book, 1993) [WorldCat.org]. https://www.worldcat.org/title/wintrobes-clinical-hematology/oclc/21558852. Accessed 11 Jul 2020

Tables

Table 1: Forward and reverse primers sequence and accession number of the studied genes

Gene	Primer sequence	Accession no.
Human MAP2	F '5-ATTTAAACAGGCAAAGGACA-3'	NR_164696.1
	R '5- TGTTGAGGTACCACTCTTCC-3'	
Rat GFAP	F '5-CGTCTGGACCAGCTTACTAC-3'	NM_017009.2
	R '5- AAG AAC TGG ATC TCC TCC TC-3'	
Human GFAP	F '5-CATGACTTTGTCCCATTTCT-3'	NM_002055.5
	R '5-GTGTGTGTGTGTG-3'	
Rat Amyloid beta	F '5-TACCCTTTAGTAGCCACT-3'	NM_000484.4
	R '5-CTA GAC AAC ACC GCC CAC-3'.	
Human CNP-1	F '5- CTGCTAGAGTGCAAGACGCTC-3'	NM_001330216.2
	R '5-CAGCCAGGTCCTCATCGAG-3'	
Rat Caspase3	F '5-AGTTGGACCCACCTTGTGAG-3'	NM_012922.2
	R '5-AGT CTG CAG CTC CTC CACAT-3'	
Rat ß-actin	F '5-TCCTCCTGAGCGCAAGTACTCT-3'	XM_032887061.1
	R '5-GCTCAGTAACAGTCCGCCTAGAA-3'	

Table 2: Water maze test

Parameters	Groups				
	I	II	III	IV	V
Latencytime (second)	17.750±1.894[c]	40.031 ± 0.921[a]	30.594 ±0.84[b]	19.107± 1.178[c]	26.781±1.785[b]
Quadranttime (second)	23.75 ± 0.796[a]	8.50 ± 0.964[c]	15.25 ± 0.620[b]	22.13 ± 0.875 [a]	16.875± .666[b]

Data were represented as Mean ± SEM.

Values within the same row with different letters are significantly different ($p < 0.05$).

Table 3: TLC and DLC of the experimental groups

Parameters	Groups				
	I	II	III	IV	V
TLC (10^3/cmm^3)	8.47± 0.33^a	6.13 ± 0.07^c	7.01 ± 0.12^b	7.9 ± 0.06^a	7.03 ± 0.09^b
Normal neutrophil (10^3/cmm^3)	3.42 ± 0.15^a	3.25± 0.09^a	3.59± 0.09^a	3.43± 0.12^a	3.28 ± 0.09^a
Toxic neutrophil (10^3/cmm^3)	0.00 ± 0.00^d	0.65± 0.10^a	0.49 ±0.04^{ab}	0.24 ± 0.04^c	0.33 ± 0.02^{bc}
Total neutrophil (10^3/cmm^3)	3.42 ± 0.15^b	3.90 ± 0.03^a	4.08 ± 0.11^a	3.66± 0.08^{ab}	3.61 ± 0.11^{ab}
Lymphocyte (10^3/cmm^3)	4.52 ± 0.24^a	2.07 ± 0.08^d	2.79 ± 0.11^c	3.84± 0.04^b	3.26 ± 0.09^c
Monocyte (10^3/cmm^3)	0.58 ± 0.10^a	0.16 ± 0.04^b	0.18± 0.05^b	0.40 ± 0.04^{ab}	0.21± 0.04^b
NLR (%)	0.76± 0.015^d	1.90 ± 0.08^a	1.47 ± 0.06^b	0.95± 0.18^{cd}	1.11 ± 0.06^c
LMR (%)	8.34 ± 1.69^a	14.00 ± 2.78^a	23.58 ± 9.59^a	10.01± 1.20^a	16.92 ± 3.94^a

Data were represented as Mean ± SEM

Values within the same row with different letters are significantly different ($p < 0.05$).

Table 4: Antioxidant and oxidative stress markers of hippocampus tissue of the experimental groups

Parameters	Groups				
	I	II	III	IV	V
CAT (U/g. tissue)	2.08 ± 0.13^{a}	0.71 ± 0.31^{b}	1.20 ± 0.03^{b}	2.01 ± 0.02^{a}	1.98 ± 0.04^{a}
GSH (mg/g. tissue)	10.49±0.62^{a}	3.99 ± 0.24^{d}	5.19± 0.45^{cd}	8.19 ± 0.42^{b}	6.59 ± 0.33^{bc}
SOD (U/g. tissue)	613.25 ±0.98^{a}	488.69 ± 1.94^{d}	485.48 ±2.54^{d}	574.53 ± 8.23 ^{b}	514.37 ± 2.07^{c}
MDA (nmol/g. tissue)	71.22 ±3.71^{d}	136.52±6.10^{a}	120.58± 3.01^{b}	82.66± 0.67^{cd}	92.18±1.15 ^{c}
NO (nmol/g. tissue	2.54 ±0.17^{d}	13.35 ± 0.79^{a}	10.60± 0.64^{b}	3.95 ± 0.16^{d}	7.04 ± 0.27^{c}

Data were represented as Mean ± SEM.

Values within the same row with different letters are significantly different ($p < 0.05$).

Figures

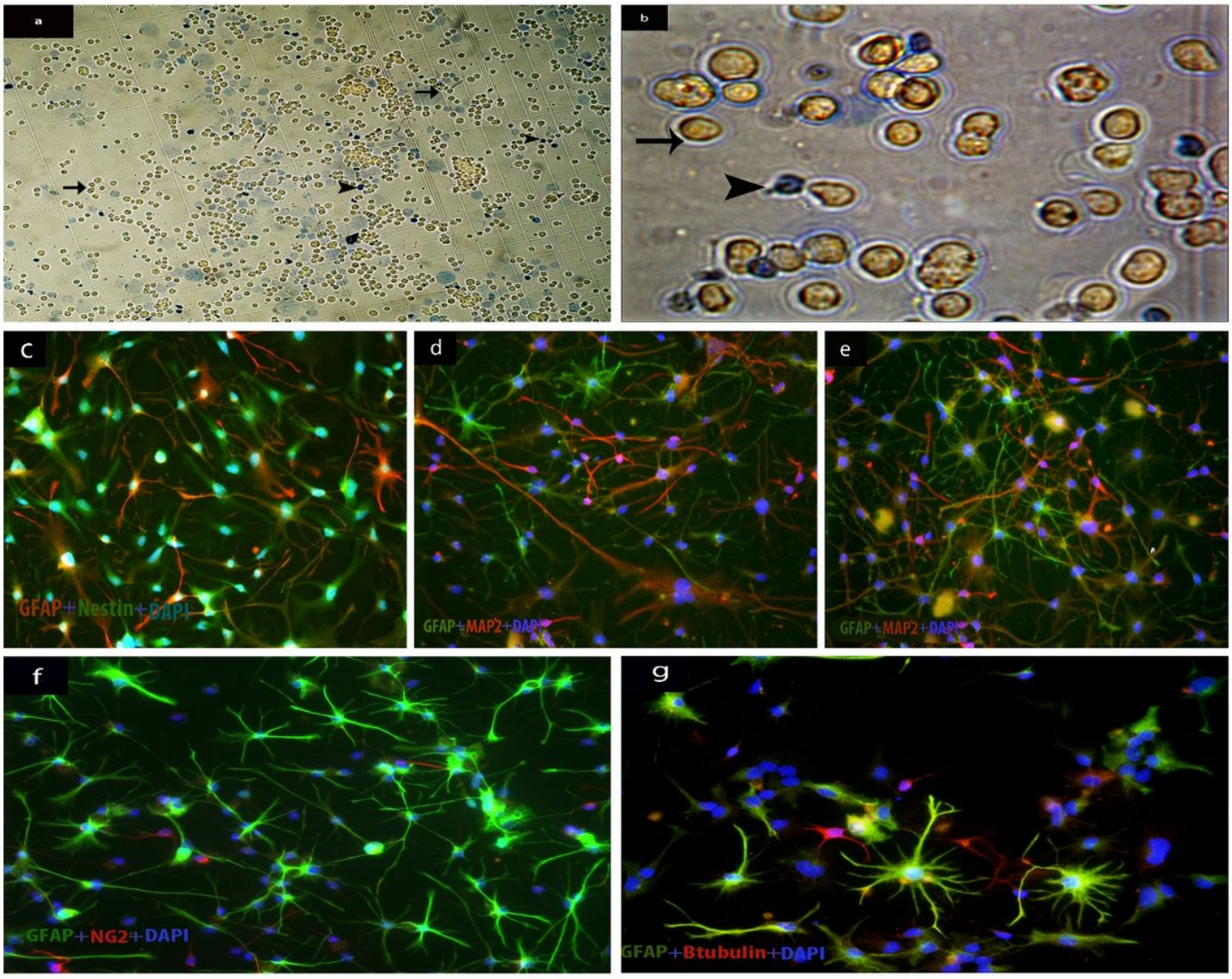

Figure 1

(a,b) Phase contrast micrograph showing single hOBNSCs during counting and viability with trypan blue exclusion test, live cells (arrow), and dead cells (arrowhead). (c,d,e,f,g): Fluorescence image (20X) hNGF-GFP-OBNSCs during proliferation phase serum-free growth media showing: The hOBNSCs were stained for the Nestin and GFAP marker (c) /MAP2 and GFAP markers (d,e) /NG2 and GFAP (f) and β-TubulinIII AND GFAP (g).

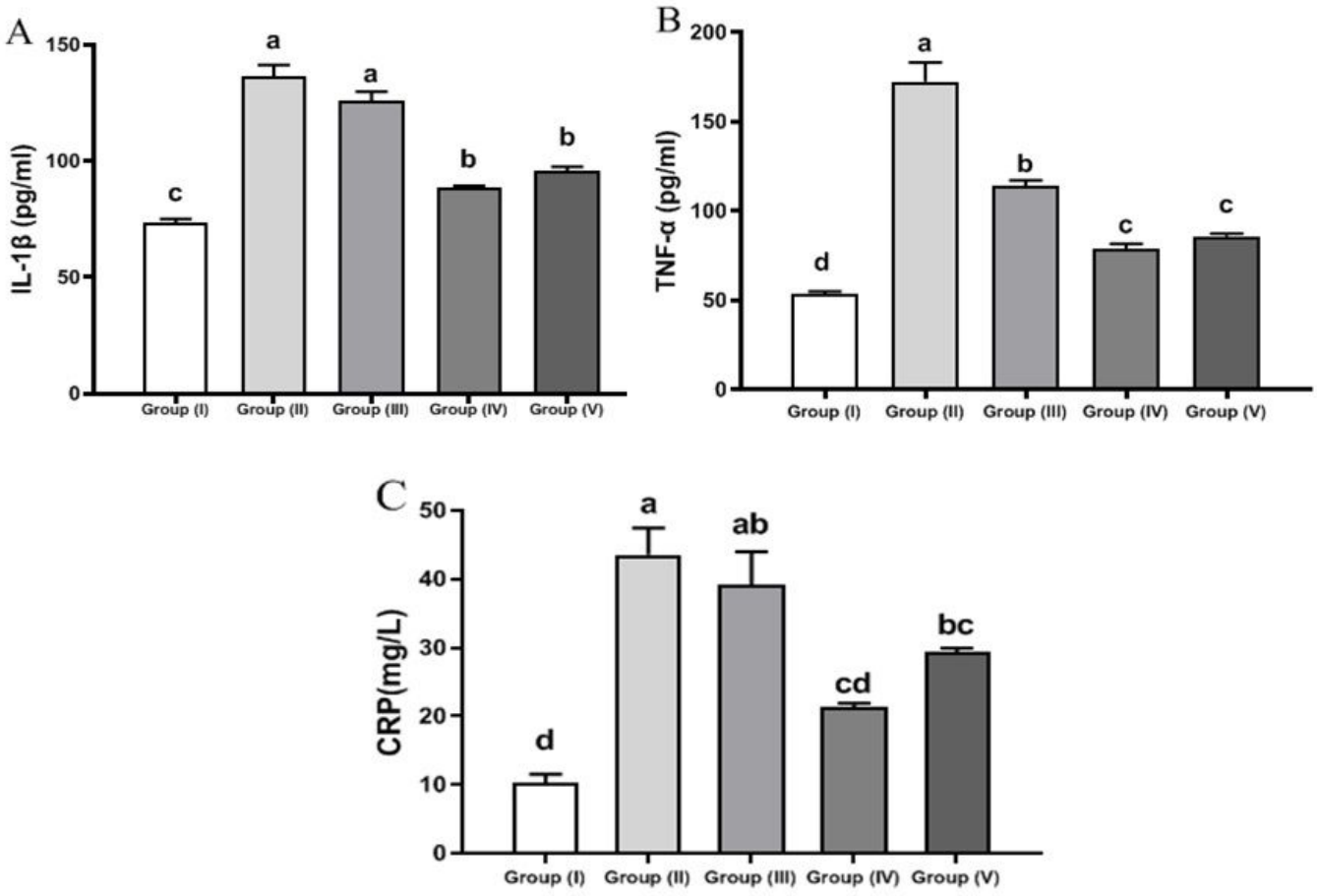

Figure 2

Serum levels of interleukin-1β (IL-1β, A), tumor necrosis factor-α (TNF-α, B) and C- reactive protein CRP, C) of albino male rats in different experimental groups. Data are expressed as Mean ± SEM. The different letters indicate a significant difference ($P < 0.05$) between experimental groups.

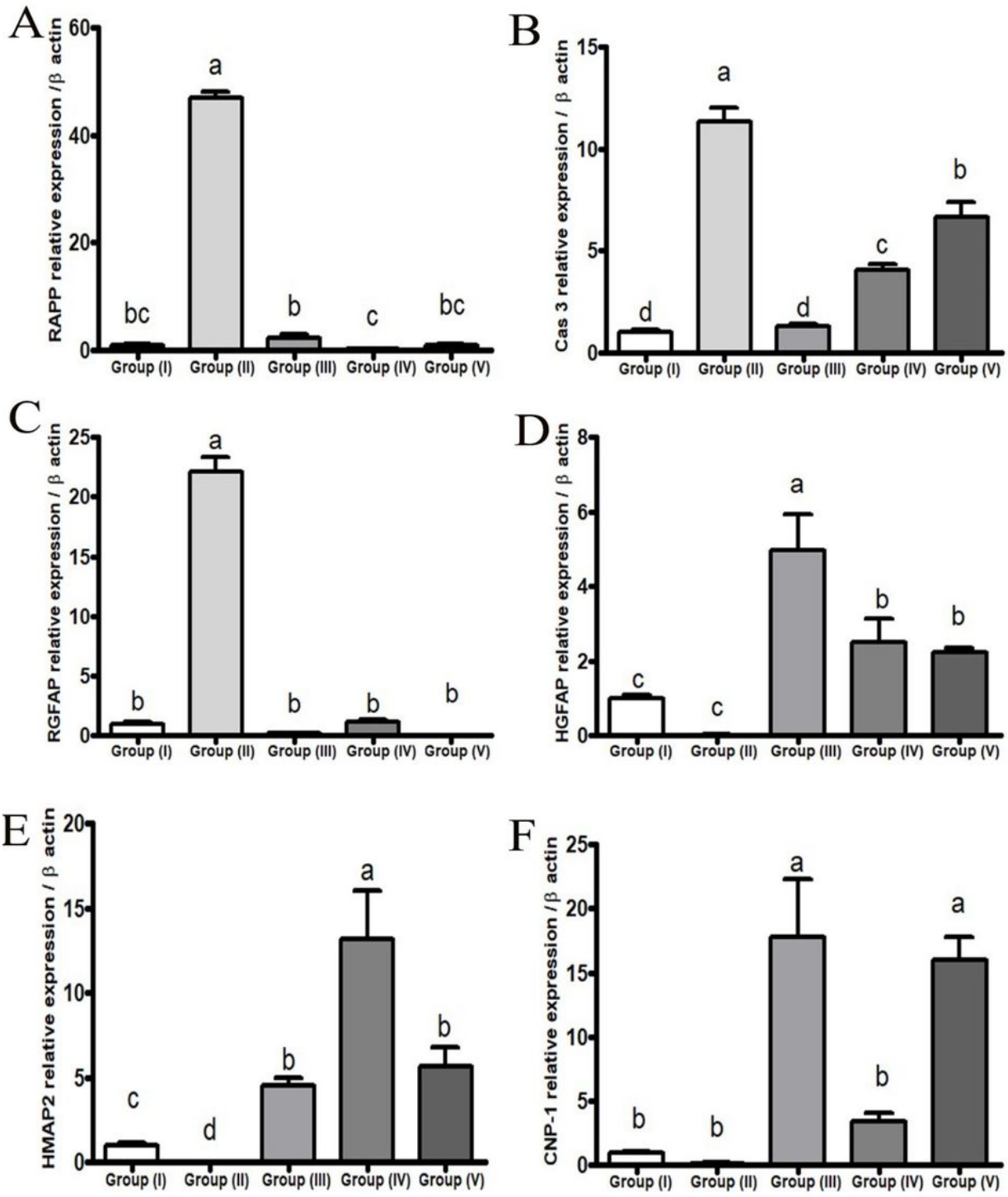

Figure 3

Relative expression of RA amyloid-beta (A), cas-3 (B), (C), RGFAP HGFAP (D), HMAP2 (E), and HCNP (F) of hippocampus tissues from albino male rats. Data are expressed as Mean ± SEM. The different letters indicate a significant difference ($P < 0.05$) between experimental groups.

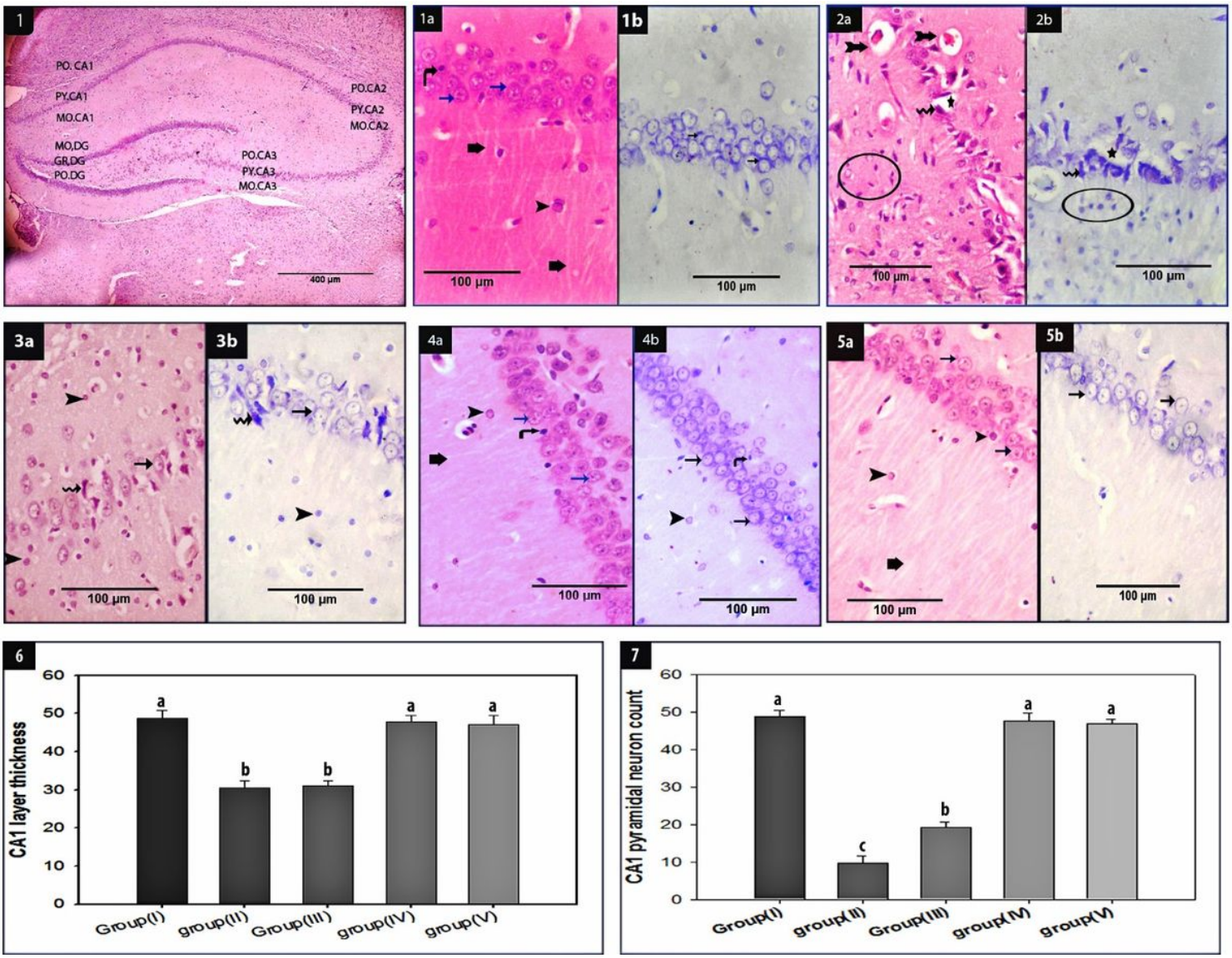

Figure 4

Photomicrograph of a section of rat's hippocampus at CA1. (1) stained with H&E showing : different fields of hippocampus, PO=polymorphic layer, PY=pyramidal layer in CA1 and CA3, MO=molecular layer, GR = granular DG= dentate gyrus.(1a.2a,3a,4a,5a) stained with H&E and(1b.2b, 3b, 4b, 5b) stained with cresayl violet showing: viable pyramidal neuron (arrow),astrocyte (arrow head),oligodendrocyte (vertical arrow), axonal tract(thick arrow),massive gliosis(inside circle),dead neurons(corrugated arrow),edema and vacuoles(tailed arrow). (6) and (7) representing pyramidal layer at CA1 thickness and CA1 viable neuronal numbers respectively, data are expressed as Mean ± SEM. The different letters indicate significant difference ($P < 0.05$) between experimental groups. 1 (group I), 2 (group II), 3 (group III), 4 (group IV) and 5 (group V).

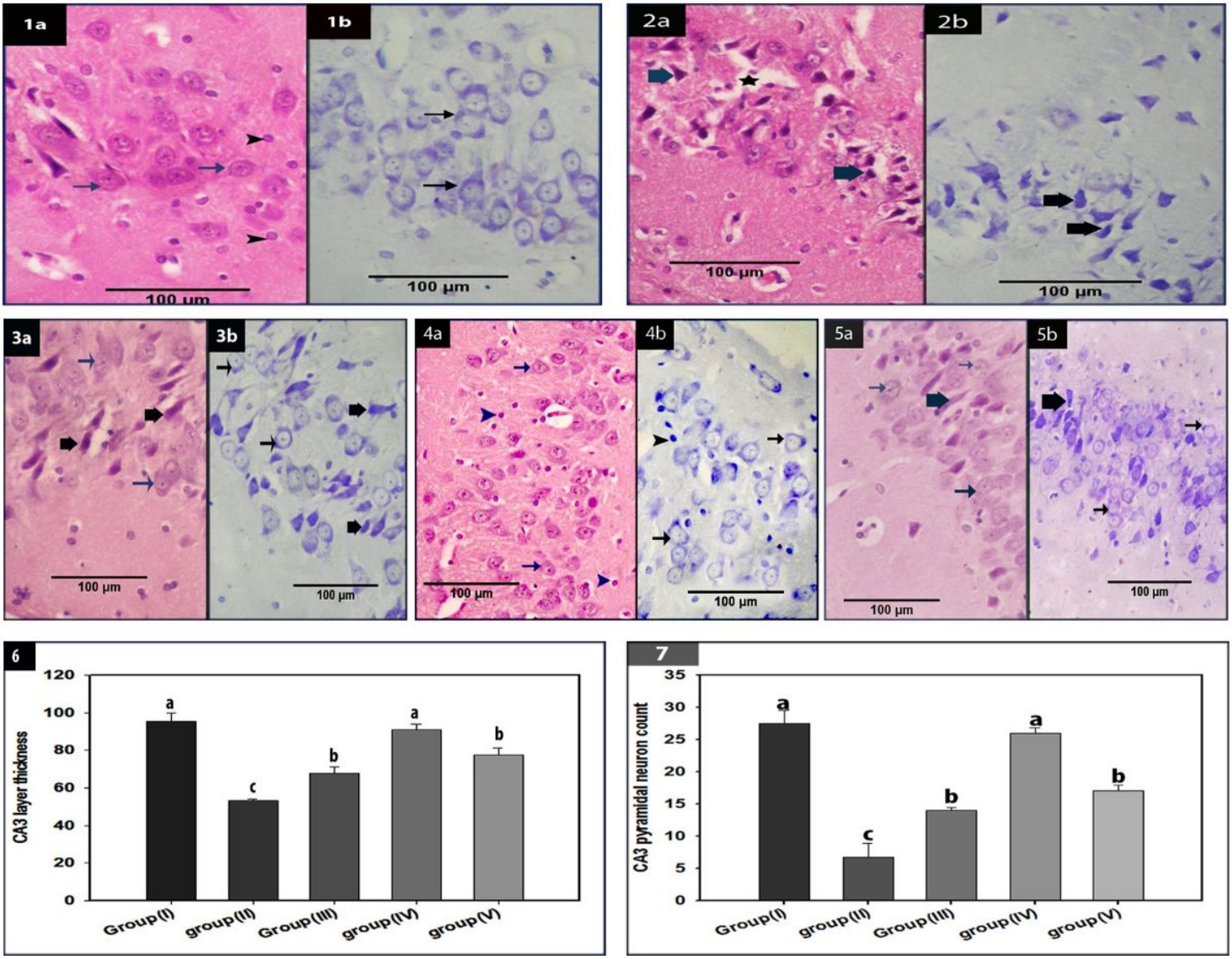

Figure 5

Photomicrograph of a section of rat's hippocampus at CA3 (1a.2a, 3a, 4a, 5a) stained with H&E and (1b.2b, 3b, 4b, 5b) stained with cresyl violet showing: viable pyramidal neurons (arrow), astrocyte (arrowhead), dead neurons (thick arrow), edema and vacuoles (asterisk) (6) and (7) representing pyramidal layer at CA3 thickness and CA3 viable neuronal numbers respectively, data are expressed as Mean ± SEM. The different letters indicate a significant difference ($P < 0.05$) between experimental groups. 1 (group I), 2 (group II), 3 (group III), 4(group IV) and 5 (group V).

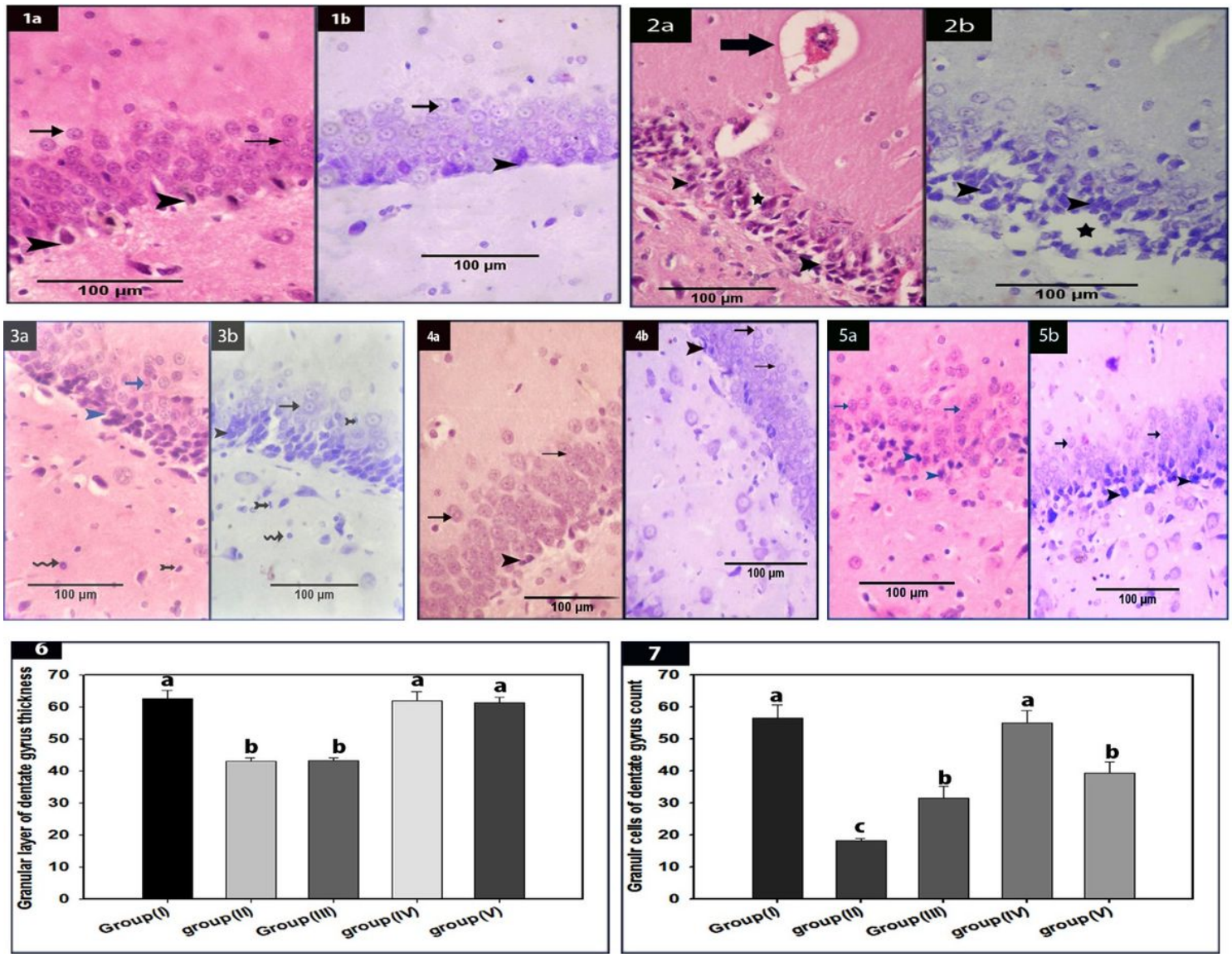

Figure 6

Photomicrograph of a section of rat's hippocampus at dentate gyrus (1a.2a, 3a, 4a, 5a) stained with H&E and (1b.2b, 3b, 4b, 5b) stained with cresyl violet showing: mature granular neuron (arrow), immature granular neuron (arrowhead), sever congestion and edema (thick arrow), disorganized granular layer (asterisk), astrocyte (corrugated arrow), microglia (tailed arrow). The granular layer at dentate gyrus thickness and viable granular neuronal numbers respectively (6, 7), data are expressed as Mean ± SEM. The different letters indicate a significant difference ($P < 0.05$) between experimental groups. 1 (group. I), 2 (group II), 3 (group III), 4 (group IV) and 5 (group V).